Informatics in Medicine Unlocked 14 (2019) 59–68

Contents lists available at ScienceDirect

Informatics in Medicine Unlocked

journal homepage: www.elsevier.com/locate/imu

CBIR system using Capsule Networks and 3D CNN for Alzheimer's disease diagnosis

K.R. Kruthika[a,*], Rajeswari[b], H.D. Maheshappa[b], Alzheimer's Disease Neuroimaging Initiative[1]

[a] Department of Electronics and Communication, Acharya Institute of Technology Bangalore, India
[b] Department of Electronics and Communication Engineering, Acharya Institute of Technology, Bangalore, India

ARTICLE INFO

Keywords:
Alzheimer's disease
CBIR
Capsule networks
Artificial neural networks
Convolutions layer

ABSTRACT

Alzheimer's disease (AD) is an irreversible disorder of the brain related to loss of memory, commonly seen in the elderly and aging population. Implementation of revolutionary computer aided diagnosis techniques with Content Based Image Retrieval (CBIR) has created new potentials in Magnetic resonance imaging (MRI) in relevant image retrieval and training for detection of progression of AD in early stages. This paper proposed a CBIR system using 3D Capsule Network, 3D-Convolutional Neural Network and pre-trained 3D-autoencoder technology for early detection of Alzheimer's. A 3D-Capsule Networks (CapsNets) is capable of fast learning, even for small datasets and can effectively handle robust image rotations and transitions. It was observed that, an ensemble method using 3D-CapsNets and convolution neural network (CNN) with 3D-autoencoder, increased the detection performances comparing to Deep-CNN alone. CBIR using the proposed model was found to be up to 98.42% accurate in AD classification. Moreover, we argue that CapsNet seems to be a promising new technique for image classification, and further experiments using more robust computation resources and refined CapsNet architectures may produce better outcomes.

1. Introduction

The imaging technologies in medical science have been developed and are undergoing technical modifications with the aim of analyzing diagnostic medical images and provide a contiguous insight of the diagnosis for the physicians and the researcher, scholars for encouragement of further researches and analysis. Various medical imaging modal techniques exist today that are involved in producing medical images, for example, Digital Radiography, Mammograms (MG), Ultrasonographs (US), MRI, Computed Tomography (CT) machines, etc. There have been many researches for the retrieval of images of the brain from the MRI databases associated with collection of brain images. A very significant advantage of the MRI scanned images are that they produce higher spatial resolutions and also, the image details are prominent for the disease diagnosis purposes. AD is a neurodegenerative disease commonly observed in old age/elderly people, manifested by gradual memory loss and impaired cognitive functions [1,2]. Its prevalence is estimated to double in the next two decades, with the aging population, thus posing a huge challenge to society [3]. The most evident character of AD pathology is neuron loss, followed by brain atrophy progressing from AD signature regions (e.g. hippocampus and amygdala) to the entire cortical region, which can be identified by the MRI scan.

These observable structural changes have happened long before a noticeable decline in cognition and thus provide an opportunity for AD early detection using image tool. For this, CBIR is the most effective image retrieval tool and it can also be very effective for managing large datasets. The systems that enable efficient image retrieval based on the image content are referred to as CBIR systems. Therefore, the working CBIR can be defined based on an image recognition task, during which the detection of key visual elements within a collection of pictures, which returns a set of relevant images. The visual features that might refer to color, texture or shape can form visual words that describe a region of a picture, are used in a visual document which describes the whole picture. A simplified breakdown of this problem would be:

a. Extract the proper visual features from an image.
b. Create a language that will describe all the AD labels.

* Corresponding author.
E-mail address: kr.kruthika@gmail.com (K.R. Kruthika).

[1] Data used in preparation of this article were obtained from the Alzheimer's Disease Neuroimaging Initiative (ADNI) database (adni.loni.usc.edu). As such, the investigators within the ADNI contributed to the design and implementation of ADNI and/or provided data but did not participate in analysis or writing of this report. A complete listing of ADNI investigators can be found at: http://adni.loni.usc.edu/wp-content/uploads/how to apply/ADNI Acknowledgement List.pdf.

https://doi.org/10.1016/j.imu.2018.12.001
Received 27 August 2018; Received in revised form 30 November 2018; Accepted 4 December 2018
Available online 08 December 2018

c. Index the collection of AD MRI images exactly like a collection of text documents.

In the recent decade, convolutional neural networks have been widely used for image classification tasks with excellent performance [4,5]. CNN related methods which are suitable for learning from a small-scale training set could be very useful for developing a classifier for AD prediction using MRI image. One of the potential solutions is using dataset transfer learning mode. This can pre-train a ConvNet on large image datasets (ImageNet), and then using the ConvNet either as a fixed feature extractor or simply as initializer.

To overcome the inadequacy and drawbacks of CNN, newly introduced machine learning structural designs known as Capsule networks (referred to as CapsNet) [6] and suitable for quick and deep learning of data images. The CapsNet is robust in accessing of data transformation and rotations, whereas requires fewer datasets for training with a lower learning curve [7,8]. There are other methods proposed for detecting AD by using different auto-encoders or 3D CNN [9,10]. This paper explores feature retrieval by integrating two different transfer learning approaches, 3D-CapsNet and a 3D pre-trained autoencoder with shallow neural networks to classify AD cases with normal healthy control based on structural brain MRI scans.

The most important property of Capsule Network is termed as “routing by agreement”, meaning that the lower level capsules are capable of predicting the results or outcomes of higher-level capsules. Thus, the activation of capsules in the higher levels correspond to the agreement of only such predictions. CapsNets not only learn good weights for feature extraction and image classification but also learn how to infer spatial pose parameters from the image. As an example, a capsule network learns to determine whether a plane is in the image, but also if the plane is located to the left or right or if it is rotated. This is known as equivariance and it is a property of the human one-shot learning type of vision [11]. This provides a visual paradigm for better explanation of the learned features. Along with these learned feature representations, we are also using a CBIR system for classification of AD while working on large datasets. Using 3D-CNN and Capsule Network from scratch with CBIR and query-based methods for calculating the F1 score. The final results are compared with the preliminary exploratory results to AD predictions.

The paper is divided into 6 different sections and topics:

Section 1 deals with introducing and providing an overview of the involvement of computer-aided diagnosis (CAD) techniques such as CNN, CapsNet, etc. in early detection of AD. Section 2 is concerned with the related works and current limitations in AD diagnosis using earlier techniques along with an overview of proposed work. Section 3 describes the methodology, experimental concepts and process of AD diagnosis. Modeling and training various components such as auto-encoder, 3D-CNN and CapsNet, etc. Section 4 briefs the results and outcome of the training and testing of the model. Section 5 beholds, the discussion on the experimental setup and compares experiment results and performances of previous works as well. Section 6 finally concludes the paper with the conclusions of the proposed work.

Our objective is to study the behavior of CapsNets in comparison to standard Convolutional Networks (ConvNets) under typical constraints of biomedical image databases, such as a limited amount of labeled data and class imbalance. We discuss the technical advantages that make CapsNets better suited to deal with the above-mentioned challenges and experimentally demonstrate their improved performance. In this paper, we demonstrate that the equivariance properties of CapsNets reduces the strong data requirements, and are therefore very promising for medical image analysis.

2. Related works

Many researches that are evident from literature, have attempted to generate automatic classifications of the structural MRIs of the brain as AD, mild cognitive impairment or normal control [12–14]. Amongst most of the common and earlier methods, VBM (voxel-based morphometry) [15], is an often used automatic tool for medical image classifications. It allows an exploration of the differences in local concentrations of gray matter and white matter. In Ref. [16], shape information in the form of spherical harmonics (SH) was used as features in the support vector machine (SVM) classifier. In Ref. [17], Statistical Shape Models (SSMs) were used to model the variability in the hippocampal shapes among the population. Hence, the image-based diagnosis of AD relied mainly on analysis of the hippocampus. The authors in Ref. [18] were able to prove that the combination of CSF amount and MRI biomarkers provide better predictions, for AD than either MRI or CSF alone.

Further, papers related to the work presented here are explained in 3 sections: Content based image retrieval for AD, 3D-Convolutional Neural Networks and segmentation for AD, CapsNet Approach for classification of AD.

As an ongoing research topic, there are not many papers available for Alzheimer disease detection using structural images from MRI and image retrieval using CBIR. The searching capabilities of the CBIR systems in medical domain are still questionable and a big research challenge. The reason is basically related to the specific nature of the medical images and subtle changes that need to be detected and taken into consideration [19]. The main concern is to find a good representation of the image content by applying techniques for feature extraction that will properly represent clinically relevant information. Subsequently, making the usage of medical CBIR systems more suitable, precise and clinically meaningful. A Neural Network was used as a multi-class identifier for the detection of different stages of Alzheimer's disease by Ref. [20]. For this, diverse techniques were used that revealed texture and contour of the hippocampus region, extracted from the MRI scans in which they used back regions of brain to check volume of AD [21]. A multi-tier technology [22] that provided ease of flexibility for experimentation with various characteristics such as, classification, feedback, representation, and ranking had an accuracy of 82.45%. The characteristic classification of inputs not only provided the estimation of stages in the disease, but also helped in adapting rankings. In a previous work, that explored different classifiers to be used in the detection and progression of AD using MRI images in building a CBIR system that was more robust is mentioned in Refs. [23,24].

The SVM was used for determining dementia or Alzheimer's in early stages by using brain structure as biomarkers [25,26]. It used 3 dimensional cross sections of the images of corpus-callosum, hippocampus, co-axial to the features of cortex for identification of AD. This technique gave up to 90.65% accurate results [27]. Deep learning techniques were capable of learning such representations from data, especially using CNN [28]. Another recent work [29] explored the utilization of deep CNNs to problems and marking use of computer aided detection (CAD) in the medical realm. The authors compared the performance of CifarNet [30] with different model training paradigms on the problems of detection or classification of lymph nodules and several types of lung diseases from CT images. They were able to augment their dataset significantly since they were using patches for training rather than full images. They concluded that transfer learning performed significantly better than training from scratch [31] and that in most tasks GoogLeNet architecture proved superior, since a more complex network is able to better learn hidden structure from data. There have also been several works using deep networks for Alzheimer's classification. In Refs. [32,33] the authors used stacked auto-encoder for AD/MCI diagnosis with up to 87.07% and 92.34% accurate results.

CapsNets are recently developed as a powerful method to overcome the limitations of CNN [6]. The 3D-CNN networks architecture is

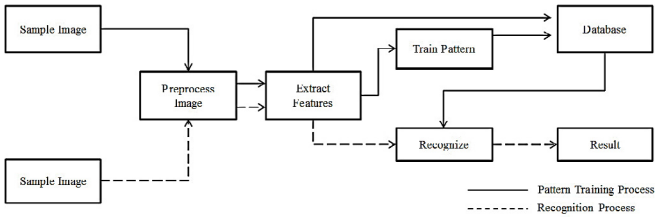

Fig. 1. Block diagram of proposed model for Alzheimer classification.

inspired by the working of the human visual system. It is somewhat, similar to the classic neural networks mainly designed explicitly on the basis of high-level feature extraction of images. A recent study implemented the CapsNet design and explored different effects of model variations, ranging from stacking more capsule layers, to changing hyperparameters [34,35]. Experimented with CapsNet and reported that CapsNet successfully overcomes CNNs for the brain tumor classification problems. They developed a visualization paradigm for the output of the CapsNet to better explain the learned features.

Moreover, there is limited availability of literature relating to CapsNets for Alzheimer's classification; hence this work is an attempt to fill the gap by introducing CapsNets for AD detection. In the following paper, we focus on the image classification problem characteristic of computer-aided diagnosis systems.

3. Methodology

The presented paper intends in utilizing classification methods by means of query-based image retrieval system, using 3D CNN and the latest benchmark technique, CapsNets to learn features. Fig. 1 shows the block diagram of the proposed model.

3.1. Data

Data used in the preparation of this article were obtained from the AD Neuroimaging Initiative (ADNI) database (adni.loni.usc.edu). The ADNI was launched in 2003 as a public-private partnership, led by Principal Investigator Michael W. Weiner, MD. The primary goal of ADNI has been to test whether MRI, positron emission tomography (PET), other biological markers, and clinical and neuropsychological assessment can be combined to measure the progression of mild cognitive impairment (MCI) and early AD. The ADNI was collectively launched by six non-profit organizations in 2003: The National Institute 139 on Aging (NIA), the National Institute of Biomedical Imaging and Bioengineering (NIBIB), the Food and Drug Administration (FDA), private pharmaceutical companies and available at adni.loni.ucla.edu. It aims to assess whether structural MRI, PET, biomarkers, as well as clinical and neuropsychological assessments can be collectively measuring the progression of MCI and early AD. ADNI has 3 phases: ADNI1, ADNI GO, ADNI2 that varied in their goals and cognitive stages in which the participants were at. The stages given in the dataset are normal control (NC), significant memory concern (SMC), early mild cognitive impairment (EMCI), MCI, late mild cognitive impairment (LMCI), and AD. The demographic information about the Standard ADNI1 1.5 T's 2 years data is represented in Table 1.

Table 1
Demographic data distribution of ADNI dataset.

Diagnosed	AD	NC	MCI
Number of subjects	345	605	991
Male/Female	186/159	301/304	646/345
MMSE ± SD	27.03 ± 2.60	21.88 ± 2.15	35.22 ± 1.24

3.2. Pre-processing of images

Dataset images are preprocessed via the software- Statistical Parametric Mapping (SPM), version 12. The standard data was preprocessed found at www.adni.loni.usc.edu website. Configuration includes: bias, noise, and global intensity normalization. The standard preprocessing process output 3D image files with a uniform size of 121 × 145 × 121. Skull-stripping and normalization ensured the comparability between images by transforming the original brain image into a standard image space, so that same brain substructures can be aligned at same image coordinates for different participants. Diluted or enhanced intensity was used to compensate the structure changes.

3.3. Building a training and learning process

This takes a two-stage approach where the first stage is to train a 3D sparse auto encoder for convolutional filter learning, the second stage implies building of convolutional neural network, in which this learned filter is used for the first layer of autoencoder.

3.3.1. Autoencoder - sparse autoencoder

An autoencoder is a 3 layered artificial neural network architecture that is used to learn unsupervised data and capable of extracting data details from an input such as dataset or an image, by accessing input data in the form of number of “small parts”, by extracting the structure hidden in the data. There is an input (encoding) and an output (decoding) layer and a hidden layer in the middle, while the hidden layer contains more or less units for a sparse and over complete representation (see Fig. 2), the input and output layers have equal units. They work by compressing the input into a latent-space representation, and then reconstructing the output from this representation.

The encoder function F maps input x to representation h, and the decoder function maps the representation h to x output. We extract 3D patches from scans as the input to the network. The decoder recreates the input data from the hidden layer h. The encoding process encodes the input with linear transform and sigmoid function,

$$h = F(W * x + b) \tag{1}$$

The sigmoid function constrains the hidden units to be in the interval (0,1), i.e. sparse vector form. While the decoder decodes the representation with linear transform and identity function. The decoder function g maps hidden representation h back to a reconstruction x'-

$$x' = g(W * h + b) \tag{2}$$

For learning it combines three terms to construct the cost function. The training is performed by optimizing the autoencoder's cost function $J(W,b)$ that depends on the autoencoder's weights W and biases b. A mean square error, for the measurement of difference between inputs and outputs of the encoder and decoder,

$$J(W, b) = \frac{1}{M}\sum_{i=1}^{M}\frac{1}{2}|x'^{(i)} - x^{(i)}|^2 \tag{3}$$

Total inputs are represented by M in the equation. There is an issue

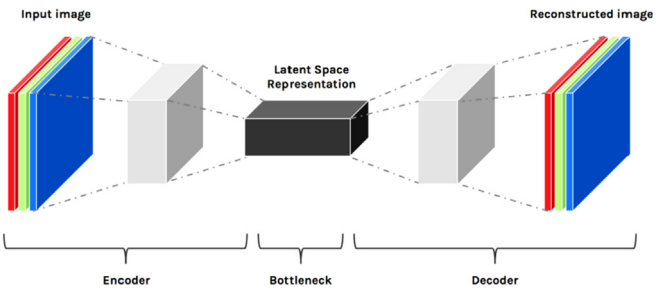

Fig. 2. Structure of an autoencoder.

that if only the reconstruction error is reduced, then it turns out to be just learning the identity function as the encoder and decoder. Therefore, an additional sparsity constraint should be imposed, i.e. the most hidden units should be closer to 0. Therefore, let s_j determine the activation mean of the hidden unit j. then s is generally a value closer to or smaller than 0 (0.05).

$$s_j = \frac{1}{M}\sum_{i=1}^{M}[a_j(x^{(i)})] \tag{4}$$

Thus, on addition of another term in penalty to function produces a s and s'_j divergence (Kullback –Leibler divergence) KL between the two. When we minimize this term, it brings s and s_j close by.

$$KL(s||s'_j) = s\log(\frac{s}{s'_j}) + (1-s)\log(\frac{1-s}{1-s'_j}) \tag{5}$$

J_2 regularization term is added to reduce the over-fitting.

$$J_2(W,b) = J(W,b) + \beta\sum_{j=1}^{h} KL(s||s'_j) + \lambda\sum_{i,j} W_{i,j}^2 \tag{6}$$

β and λ are two hyper-parameters that controls the amount of the last two terms. The input of our autoencoder is the small patches extracted from the MRI scans. Fig. 3 shows a 2-way architectural classification of neural network.

3.3.2. Training of 3D sparse autoencoder

The 3D sparse autoencoder extracts features from a $7 \times 7 \times 7$ patch of the 3D MRI scan, and transfer each patch-feature into a sparse vector with size of 410. To train the autoencoder, we used 300 3D MRI scans from the training dataset and randomly mined 1000 $7 \times 7 \times 7$ patches from each of the 3D scan. Empty patch (sum of all the voxels in the patch is zero) was replaced with a new draw. The autoencoder was trained through 250 epochs.

3.4. Training the 3D-CNN

The second stage in the process comprises of training the 3D-CNN. The CNN we use in this project has one convolutional layer, one pooling layer, two linear layers, and finally a log softmax layer. Weights *(W)* and other biases *(b)* of the encoder from trained model of autoencoder are transferred to a 3D filter of 1st –convolutional layer of 3-Dimensional-CNN.

In place of connecting all possible pixels with each neuron, we recommend a 2D open region known as 'receptive field [35]' (7×7 in the spatial dimension and 3 in the temporal dimension with 3 color channel inputs) that extends to the whole input depth ($7 \times 7 \times 3$), it is here MRI for AD image pixels are finally connected to the input layer of the neural network. Fig. 4 shows 2d and 3d convolutions. In these regions of network layer cross-sections (each comprising of numerous other neurons) operate.

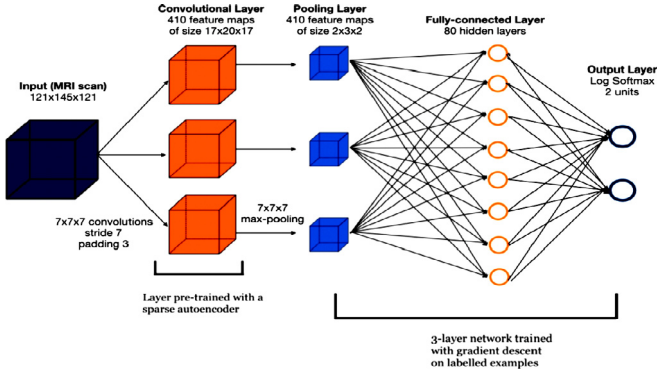

Fig. 3. 2-way architectural classification of neural network.

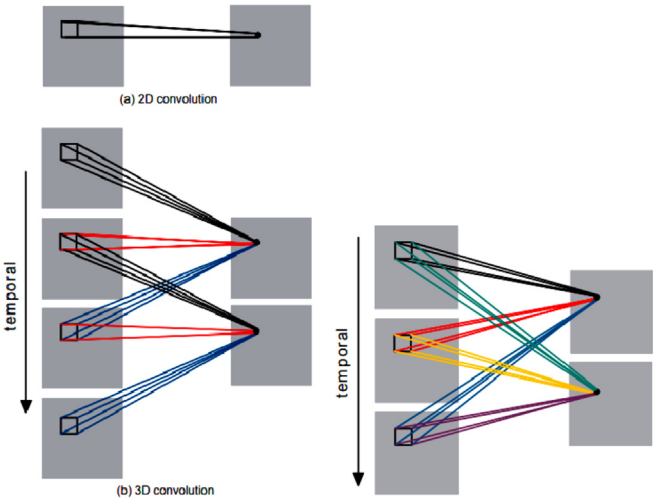

Fig. 4. 2d and 3d convolutions.

Spatial relationships employed by the CNNs decreases parametric numbers of learning, hence, which further improve the training process in back-propagation and feed-forward curves. Error in back-propagation E defines an error function, with input x, ith, jth neurons as y, while a and b are indices, l is layer number, w is filter weight, number of neurons of a layer as M whereas m is the size of the filter.

$$\frac{\delta E}{\delta y_{ij}^{l-1}} = \sum_{a=0}^{m-1}\sum_{b=0}^{m-1}\frac{\delta E}{\delta x_{(i-a)(j-b)}^{l}}\frac{\delta x_{(i-a)(j-b)}^{l}}{\delta y_{ij}^{l-1}} = \sum_{a=0}^{m-1}\sum_{b=0}^{m-1}\frac{\delta E}{\delta x_{(i-a)(j-b)}^{l}}w_{ab} \tag{7}$$

Nevertheless, convolutional neural networks have successfully achieved to outrun various methods in image retrieval processes, they still conflict with certain disadvantages. For example, affine transformation is not handled robustly, also, they lack to consider the spatial relationships and features within the images. Apart from this, CNNs are incapable of producing accurate outputs and lack performances in the presence of small datasets, relating to most of the brain MRIs or other database images. Hence, CNNs require datasets that include all kinds of spatial rotations and transformation produced for the training purpose to aid in the improvement of their coherent generalizations.

The CNN architecture we used, has been illustrated in Fig. 3. Besides, we added dropout layers with percentage 50% to prevent the model overfit. The 3D arrangement of the neurons over the input layer performs the convolution operations. We took 80% of our data as training data, and another 20% as testing and validation data for 250 epochs. Loss values of the epochs is shown in Fig. 5.

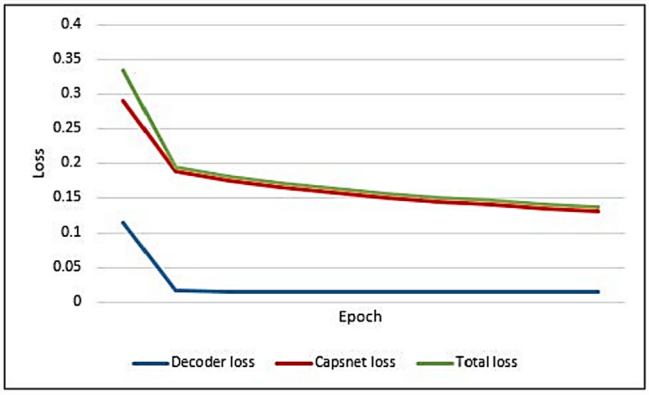

Fig. 5. Loss values of epochs in proposed architecture.

3.5. CapsNet or capsule network

The capsules in a Capsule Network are generally groups of neurons. These act in such a manner, that different parametric poses are represented by activity-vectors of these neurons, whereas, the lengths of the vectors represent the respective probability of existence of a spatial feature. Generally, the shortcomings of a CNN are mostly connected to the presence of pooling layers. However, layers in CapsNet are significantly replaced with a more appropriate criterion known as "routing by agreement." On the basis of these criterion, the resulting outputs generated in the first layer are transmitted to the parent-capsules of next layer. Although, the coupling-coefficient of the capsules are not similar. Here, all the capsules try to perceive the outputs of the parent-capsules. The coupling-coefficient among these two capsules is increased, based on the prediction conformations to the actualized outputs of the parent-capsules. Thus, if we consider u_i as the outputs of capsule i, it's detection for parent-capsule j is calculated by:

$$u'_{j|i} = W_{ij} u_i \tag{8}$$

Where $u_{j|i}$ represents the prediction-vector of output of the jth capsule in a higher level, which is calculated by capsule i in the subsequent layer. W_{ij} is the weighted coefficient matrix that is learned in the backward process. Thus, on the basis of the degree of conformations among below layer and the parent capsules, the coupling coefficient c_{ij} can be computed from the equation:

$$c_{ij} = \frac{exp(b_{ij})}{\sum_k exp(b_{ik})} \tag{9}$$

Here b_{ij} is the probability of log, for determining if capsule i should be linked to the capsule j, also, it is initialized to zero at the very start of the procedure. Hence, the input-vector to the parent-capsule s_j will be computed as below:

$$s_j = \sum_i c_{ij} u'_{j|i} \tag{10}$$

Ultimately, the following subsequent function is utilized to prevent the capsules' outputs from going beyond '1', generating the final outputs of each capsule on the basis of their initial vector values defined:

$$v_j = \frac{||s_j||^2}{1 + ||s_j||^2} \frac{s_j}{||s_j||} \tag{11}$$

where s_j is the capsule j's input vector and v_j is its output. The probability of log updates is frequent in this type of routing process i.e. based on the agreements between v_j and $u_{j|I}$ utilizing the facts of the two agreeing vectors, will have a larger inner product. Thus, agreement a_{ij} for the update of log probability and coupling-coefficient is computed by:

$$a_{ij} = v_j . u'_{j|i} \tag{12}$$

Loss function l_k for every capsule k in the terminal layer, which targets high-loss values on capsules with long output instigation parameters when the presence of any entity is not recorded. The loss l_k is calculated by:

$$l_k = T_k \max(0, m^+ - ||v_k||)^2 + \lambda(1 - T_k)\max(0, ||v_k|| - m^-)^2 \tag{13}$$

where, in the presence of class k (whenever it is), T_k is 1, otherwise it is 0. The terms λ, $m+$ and $m-$ are the significant parameters that are to be confirmed earlier during the beginning of the learning procedure. Actual capsule network architecture is presented in Ref. [36] that consisted of a single layer of convolutional filters and two layers of capsules. Exceedingly, it had 3 layers of interconnected neurons that tried to re-construct the inputs using the instantiation parameters from the capsules related to the true labels.

3.5.1. Designing CapsNet

As we went through several architectures of network in capsule network, we considered building a model approach as closely similar to the one mentioned in the original papers. Only the difference here is that the original model had only 64 feature-maps in its convolutional layers, whereas, our proposed model has 256 features. Layers of the proposed model can therefore be summarized as following:

- The MRI images are taken as input that are down-sampled to 64 × 64 from 512 × 512, for reduction of parameters and to decrease the time taken during training.
- The second layer is a primary capsule layer consists of 32 channels for convolution where each capsule consists of 9 × 9 kernel and the value of stride being 2. This is also same as the original paper proposed by Hilton [6].
- The final layer comprises of three capsules, also known as "Class Capsules," for each class type defined for AD, this includes AD, MCI and NC as they are three classes of Alzheimer that we are using. The dimensions of these capsules are 16.
- The decoder segment contains 3-interconnected layers comprising of neurons say 512, 1024 and 4096. It is examined that neurons in the input layer are same as the number of image pixels in the output layer minimizing the re-construction loss.

We can see in our different test experiments, that our network performed really well using the large dataset of ADNI, but due to the risk of overfitting and underfitting we have to make use of an algorithm called early stopping [37]. According to this the training process is continued to the point that accuracy of validation begins to drop at the end of each epoch during the training of model.

3.5.2. Experimental setup

For the purpose of testing our proposed approach, we utilised the datasets mentioned in Section 3.1. Fig. 6 shows the mean square error (MSE) while calculating on samples. The mapping from the AD data to the capsule features is important for the next reconstruction. The mean square error on testing samples is close to that on the training samples. This indicates, that our proposed method avoided the over-fitting, because of the dimension-decreasing operations and the capsules including the feature information of equivariance. The performance will get improved when obtaining more AD classification data.

Using our own architecture of capsule which we changed in regards to Ref. [6], where we used convolution networks with 64 features. This makes the network stronger as the image reconstruction encourages the network to consider vectors of capsule as real entities before regenerating and encoding in each MRI image.

Apart from the original paper, we implemented this ADNI dataset with the translation invariance which means that our model will be able to detect the image even if they are not in their correct relative positions. This is unlikely of CNN, and hence CapsNet with CNN was analyzed by us for AD classification. Fig. 7 demonstrates the results of CapsNet and CNN comparisons. Further, on the basis of these results, it is observed that capsules network performs way better than CNN as the dip in loss for capsule is lower for the current data. As mentioned

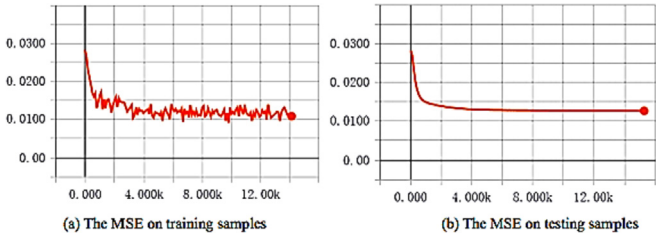

Fig. 6. The learning curves during training for AD classification (MSE - mean square error).

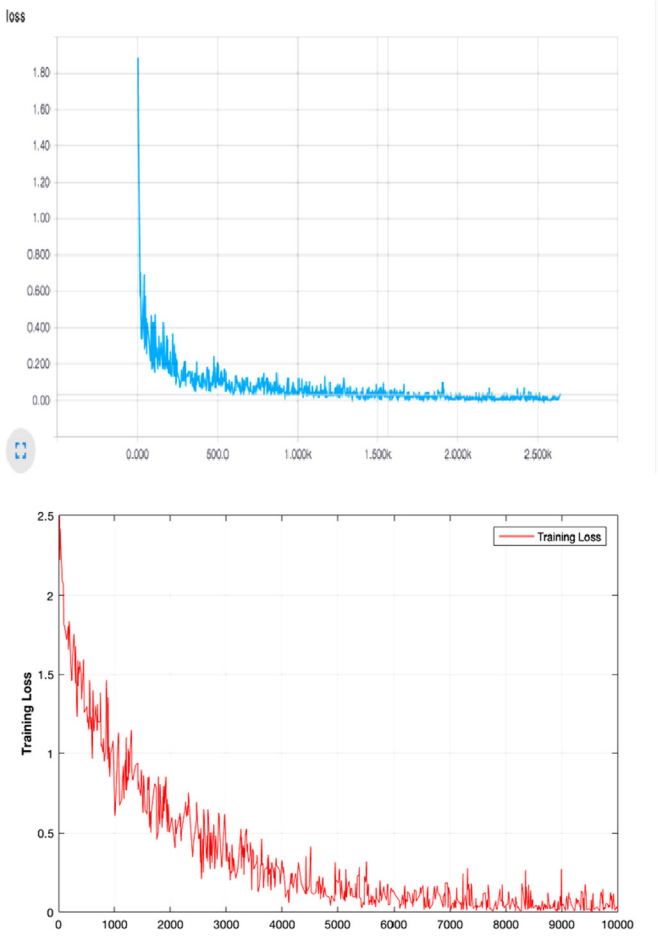

Fig. 7. Training loss values of each epochs. Capsule Network (Blue) and CNN (Red).

earlier, the capsules tend to acquire every detail within the input image, even from backgrounds. Taking the facts into consideration MRI scan image of the brain is taken from varied angles, therefore, sagittal and coronal interference contain many stochastic changes.

3.6. CBIR

The promising results of deep neural networks in Alzheimer Detection and the success of the CNNs are making CBIR famous. The change in the usual BoVW process [38] is that features are extracted by a CNN, which has been previously trained on image data, thus replacing the handcrafted feature extractors like SIFT. The activation vector to a specific point inside the 3D convolutional layer activation map is used as its feature descriptor, with high dimensionality depending on the kernel's hyper depth. The regions of interest have typically a fixed square-shaped size and their center points are evenly arranged, forming a grid on the MRI image. The work focuses on capitalizing the achievability of such benefits and adopting the proposed model for Alzheimer's detection. Along with this, we also build a query based CBIR which proposes to take a query image, for the classification using the two models, and retrieves five similar images to aid pre-diagnosis and progression of AD.

Apparently, methods, creation, indexing and retrieval can remain the same in both CNN-based and Capsule-based image retrieval systems. Multiple tasks are combined in a pipeline of processes with various methods from the domains of Machine Learning, Data Mining and Information Retrieval. These can be described by the following workflow of steps:

1. Supervised training of a deep neural network (DNN), which is typically a CNN or CapsNet. This is performed on an image collection with annotations like class labels of Alzheimer Detection (NC, MCI, etc.). The learned parameters of the network will integrate the feature extraction capabilities and its layers will act as feature extractors.
2. An image is recalled through the pre-trained model. The output activations of a selected layer are the feature descriptors for the image regions. Different layers correspond to different scales of the image resolution.
3. The feature descriptors for Alzheimer Detection are quantized to create a Visual Feature Library (VFL) that is specific for
   a) The trained state of the DNN architecture,
   b) The ADNI image dataset used for training and
   c) The selected neural network layer (3D CNN and Capsule Network).
4. The image regions are described by visual words of the VFL. Each word is a representation of a region's features.
5. Visual documents can be indexed by a search engine and retrieved by queries, using standard text IR methods. The tasks of image classification for AD can be ported as image retrieval tasks on VFL representations. Retrieving an image of the same class in the top rank can be equivalent to the classification. The image areas can be segmented and indexed as different fields in the CBIR system. A fielded search with an image of an object can detect it and localize it inside the returned set of relevant images.

3.6.1. Retrieval performance

The Precision and Recall method, which is most frequently utilized for performance analysis of CBIR, is proposed for the framework of CBMIR. Precision is calculated as the ratio of total relevant images retrieved to the total number of images retrieved. Recall R on the other hand, is represented by, the ratio of total relevant images retrieved to the total number of relevant images in the database. F1 score from the mathematical expression is therefore:

$$P = \frac{TP}{TP + FP} \tag{14}$$

$$R = \frac{TP}{TP + FN} \tag{15}$$

$$F_1 = 2\frac{TP \times R}{TP + R} \tag{16}$$

For a content-based image retrieval experiment of the query set, 1 image each for the 3 classes (NC, MCI,AD) was used. Even though the models (CNN and CapsNet) learned state do not generalize adequately, these classes have a fair F1-Score and are close to the 50 samples per class limit. This selection ensures a good representation of relevant topics in an imbalanced image collection like ADNI dataset. For retrieval experiments 3 random images from the ADNI dataset compose the random query images.

Nevertheless, an interesting observation is made on the retrieval results when querying the image collection with the completely unknown MCI images. The Capsule Network performs better for hand-picked images than for randomly selected images from CNN. This could be based on the fact that the weights are more discriminative to the global visual characteristics of a class, or simply caused by the different frequency distribution of the visual words.

4. Experimental setup and results

4.1. Experimental setup

As configuration we have a DELL laptop with 16 GB RAM, Ubuntu 16.04LTS OS and Nvidia GeForce Graphics/GPU with Python 2.7 and Keras software installed. Significant classification and accuracies were

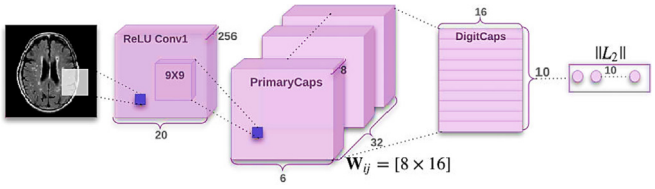

Fig. 8. Schematic representation of the CapsNet architecture.

accessed on ADNI database (see Table 3), as target domain, for the MRI image detection of AD/MCI/NC. Classification detection accuracies were estimated for the tests by cross-validation method. Accounting to time limits the epochs were set to 100. About 25% data was set to test and 75% to training. Additional images were added to the data as non-diseased, for superior detection and classification of the AD, MCI, NC. Fig. 8 gives a schematic representation of the CapsNet architecture for the experiment.

Our experimental setup of the 3D-CapsNet utilizes instantiation parameters. Adam is used for the optimization and training vice-versa. ReLu is at inner layers and softmax with fully connected top-most output layer, for the detection of an input brain structural Magnetic Resonance Imaging (sMRI) to any of the AD, MCI, or the NC subset.

4.2. Results

CNNs have been best suited for layer-pixel pooling mode of image transitions, accessing data in the form of multiple arrays. This relay data information received as input from layer to layer, also known as routing. Nonetheless, CNNs generally require a fairly large number of datasets to process for training, but are unable to manage the input data transformations properly and overlook vital details at times. CapsNet [6] is a novel introduction in the machine learning process structural design to outperform the drawbacks of the convolutional CNNs, & proposed to revolutionize the deep learning process. CapsNet require fewer dataset for training as compared to CNNs. The CapsNet processes medical MRI image dataset and handles more efficiently with robust dynamic routing, related to specific characters (size, location, orientation, etc.) and rotations, concerning medical details.

The study employed 3D-CapsNet and found it to be more robust (94.06%) accuracy for Alzheimer Disease detection over CNNs and other architectures discussed in the paper. We trained our proposed architecture for 100 epochs and computed the results, it was seen that in the initial stages the training was faster and the total variable loss depended on the CapsNet loss. Moreover, CapsNet model can aid medical research fellows in great deal for obtaining accurate and efficient outputs. Also, CapsNet is capable of handling large datasets with low training turns and small sample sizes, which is the reason for its success.

5. Discussions

Computer vision and learning technology are gaining remarkable, innovative approaches and improving with improved schematic architectures. Convolutional neural networks (CNNs) have been employed by researchers and engineers extensively in solving general problems in classifying image, with prominent good results on different image types [39]. Although CNNs are successful at identifying features of images, using convolutional layers, they also have many limitations. CNNs use deep learning and registered successful impact in a wide-range of applications related to shapes, edge detection and classifying images from datasets [40].

ConvNets (CNNs) lack orientation perspective or failed to set relationship between spatial information such as orientation, size, position, perspective, etc. This is due the fact that CNNs process data information between the layers using max-pooling sub-sampling method [41]. CNNs require large datasets for the training and this means time and resources too.

Table 2
Relative comparison of CNNs and CapsNet.

S. No.	Condition	Convolutional (CNNs)	Capsules Network (CapsNet)
1	Training Data	Large datasets	Small datasets
2	Routing	Max-pooling subsampling	Dynamic routing-by-agreement
3	Input-Output	Scalar value	Vector value
4	Detection of Spatial information	No	Yes
5	Accuracy	Less accurate	More accurate
6	Affine transformation handling	No	Yes

These are susceptible to various other adversarial attacks [42]. To eliminate the limitations and overcome the shortcomings of CNNs, a new algorithmic approach was introduced recently as CapsNet [43]. CapsNet employs the dynamic routing between capsules [44]. These use vector-input/output values contrasting to CNNs that use scalar-input/output values and requires small-data for training. The max-pooling sub-sampling is replaced by the new routing-by-agreement method. Table 2 shows a relative architectural comparison of CNNs and CapsNet.

In short, the CapsNet is efficient in providing spatial relationship between the features of the image and understanding changes in shape, size, position, orientation, luminance, perspective, etc. through the robust routing and handling affine transformations for the image classification. CapsNets cover more of the image features and regions than CNNs. Thus, CapsNet has found to outperform CNNs in many image classifications, accuracy, low training data, and is subject to perform even better on fine-tuning of parameters of supply datasets. Combination of different techniques such as autoencoder, Convolutional CNNs, and CapsNet can increase accuracy and efficiency.

A comparison accuracy of current work and earlier experiments is highlighted in Table 4.

Through this experimental study it can be related that the CapsNet outperforms Convolutional Neural Networks (ConvNet) in classification and detection of the AD. Comparison of other architectural approaches with the similar data and setup were performed for accurate detection of AD/MCI/NC. It was observed that CapsNet clearly outperforms different ANN approaches with better performance and classification.

5.1. Comparison of different schema

5.1.1. 3D-autoencoder

The 3D-autoencoder with a shallow neural network performs well as we expected. The classifier achieved a training accuracy about 86%, but with about 92.61% validation accuracy for AD vs NC > Recall that the 3D-autoencoder was pretrained on about 2000 3D-image patches from the training dataset, the 3D-autoencoder may extract not only the AD specific features but also lots of image specific characters which make the subsequent neural network can easily memorize the training dataset. For further improvement, some augmentations could be added to the patch images for the auto-encoder training. In addition,

Table 3
Statistical data of 225 subjects (source: ADNI).

	AD	MCI	NC
Total subjects	75	75	75
Gender (Male/Female)	40/35	52/24	39/35
Age (mean ± STD)[a]	75.5 ± 8.0	76.9 ± 7.5	75.6 ± 6.2

[a] STD = standard deviation.

Table 4
Comparison (Accuracy %) of related works in literature with proposed ANN.

Approach	Modalities	AD/MCI/NC	AD/NC	AD/MCI	MCI/NC
Suk et al. [45]	PET + MRI + CSF*	$n/a^{\#}$	$95.9_{1.1}$	n/a	$85.0_{1.2}$
Zhu et al. [46]	PET + MRI + CSF	n/a	$95.9_{n/a}$	n/a	$82.0_{n/a}$
Zu et al. [47]	PET + MRI	n/a	$96.0_{n/a}$	n/a	$80.3_{n/a}$
Suk et al. [48]	PET + MRI	n/a	$95.4_{5.2}$	n/a	$85.7_{5.2}$
Liu et al. [10]	PET + MRI + CSF	$53.8_{4.8}$	$91.4_{5.6}$	n/a	$82.1_{4.9}$
Hosseini et al. [49]	MRI	n/a	$91.4_{1.8}$	$70.1_{2.3}$	$77.4_{1.7}$
Liu et al. [9]	MRI	n/a	$93.8_{n/a}$	n/a	$89.1_{n/a}$
Zhang et al. [50]	PET + MRI	n/a	$83.1_{1.4}$	$69.6_{n/a}$	n/a
3D-CapsNet	PET + MRI	$\mathbf{89.1}_{1.7}$	$\mathbf{97.6}_{1.0}$	$\mathbf{95}_{1.8}$	$\mathbf{90.8}_{1.1}$

Table 5
Accuracy and ROC of different combinations of the stages of Alzheimer using 3D –autoencoder.

Category	Accuracy	ROC
AD vs NC	93.21	0.98
AD vs MCI	94.06	0.91
AD vs NC	88.37	0.86

incorporating image patches that not belong to brain MRI scans may also help to improve the generalizability of the auto encoder to avoid overfitting. The accuracy we get on the validation set is 92% for AD vs NC. Table 5 shows the ROC values of 3-way classification using 3D CNN.

5.1.2. 3D-CapsNet

CapsNet performed the best in all cases with a validation accuracy of 94.06% for AD vs NC. Going forward with our architecture, cross-validation results are very promising it is probably safe to speculate, that a computer-aided decision system, which would help to diagnose Alzheimer disease faster and more accurately, can be envisaged in a near future. By re-routing how vectorials work, working out degree co-relativity and changing interplay of propagation. Table 6 outlines the obtained results for Alzheimer classification accuracy based on different Capsule network architectures. We chose the best Architecture to go forward with classification. Table 7 shows classification accuracy for 3 classes. By looking at these results of changing networks we can see that, reduction of a 256 feature-maps from 256 to 64 features-maps (original-schema), produced higher accuracies. We evaluated the total-loss in a network, composed of two parts: CapsNet-loss and Decoder-loss. We can now speculate that the result by CNN is less accurate than CapsNet, this generally happens because of relative routing algorithm (routing by agreement) that work with vectors. Due to the degree of co-relativity and changing interplay of propagation we managed to stack more layers of sub-sectioning layers for our AD Classification.

Table 6
Alzheimer classification accuracies on the basis of various CapsNet architectures.

CapsNet Architecture	Prediction Accuracy
Original schema	82.30%
Two convolutional layers with 64 feature-maps each	82.01%
64 feature-maps with 1 convolutional layer	94.6%
64 feature maps and 16 primary capsules with 1 convolutional layer	83.61%
64 feature maps and 32 primary capsules of dimension 4 with 1 convolutional layer	92.07%
Three fully connected layers with 1024, 2048 and 4096 neurons	83.93%

We chose the best architecture (CapsNet) to go forward with classification process.

Table 7
Classification accuracy of different of stages of Alzheimer using Capsule Network.

Category	Accuracy
MCI vs AD	94.6%
NC vs AD	92.98%
NC vs MCI	94.04%

5.1.3. CBIR

With the F1 score, we can see that both models did perform well, although here as well Capsule network got ahead. We can now check in our query-based retrieval system of how a test image will yield most similar images of that class. However, many other retrieval systems can be tested to bring higher accuracy in retrieval. It is though safe to speculate that instead of hand-picking the images from the cluster, image retrieval of computer aided system using the new model is a quite promising. With this, medical researchers can be aided much efficiently and accurately. We trained the proposed architecture for 100–250 epochs and calculated the 3 losses at the end of each epoch. The CapsNet model can aid medical research fellows in great deal for obtaining accurate and efficient outputs. Also, CapsNet is capable of handling large datasets with small training sessions and sample sizes, which is the reason for its success. Table 8 shows an F1 score of different models that we have used in our paper for CBIR.

6. Conclusion

This work has sufficiently addressed the problem of discovering well performing Capsule-based features for increased CBIR performance. The experimental results showed adequate performance of the overall model. The algorithm is fast, simple for the Alzheimer classification and suitable for low computational resources. Nevertheless, the evaluation system used for experiments could be considered a systematic approach to CBIR research. Moreover, the complexity is fully explored and the factors that contribute to the CBIR. With a good F1 score of both models we can be sure that it can be implemented in an efficient manner. Our results suggested that transfer learning is a potential suitable approach for training CNN classifier on a small-scale training dataset for AD prediction based on structural brain MRI scans. Also, through this work, we explored the efficiency and utility of the CapsNets for identification of AD. Output of capsules being vector values, use of efficient dynamic routing method ensures better accuracy of CapsNet over all other architectures. Since, these networks can function with small training samples, and high equivariance, Capsule network overrides CNNs in AD classification. In the future, we plan to analyze the effects of using more capsule layers on the classification accuracies. Also, while comparing with the other methods, we have seen that our method produced promising results.

Acknowledgements

Data collection and sharing for this project was funded by the AD Neuroimaging Initiative (ADNI), National Institutes of Health Grant U01 AG024904 and DOD (Department of Defense award number W81XWH-12-2-0012). ADNI is funded by the National Institute on Aging, the National Institute of Biomedical Imaging and

Table 8
Results showing different F1 score for CNN and Capsule models used in CBIR.

Method	F1 measure
3D CNN on whole training set	97.85
CapsNets on whole training set	99.76

Bioengineering, and through generous contributions from the following: AbbVie, Alzheimer's Association; Alzheimer's Drug Discovery Foundation; Araclon Biotech; BioClinica.; Biogen; Bristol-Myers Squibb Company; CereSpir, Inc.; Cogstate; Eisai.; Elan Pharmaceuticals.; Eli Lilly and Company; EuroImmun; F. Hoffmann-La Roche Ltd and its affiliated company Genentech, Inc.; Fujirebio; GE Healthcare; IXICO Ltd.; Janssen Alzheimer Immunotherapy Research Development, LLC.; Johnson Johnson Pharmaceutical Research Development LLC.; Lumosity; Lundbeck; Merck.; Meso Scale Diagnostics, LLC.; NeuroRx Research; Neurotrack Technologies; Novartis Pharmaceuticals Corporation; Pfizer.; Piramal Imaging; Servier; Takeda Pharmaceutical Company; and Transition Therapeutics. The Canadian Institutes of Health Research is providing funds to support ADNI clinical sites in Canada. Private sector contributions are facilitated by the Foundation for the National Institutes of Health (www.fnih.org). The grantee organization is the Northern California Institute for Research and Education, and the study is coordinated by the Alzheimer's Therapeutic Research Institute at the University of Southern California. ADNI data are disseminated by the Laboratory for Neuro Imaging at the University of Southern California.

Further, the authors would like to express their sincere gratitude to Dr Akshay Pai, for his assistance in obtaining the data and support for experimentation of the work. Also, Authors are thankful to Prof. B.A. Patil and Think and Ink Education and Research foundation for guiding to carry out this work.

References

[1] Langa Kenneth M. Is the risk of Alzheimer's disease and dementia declining? Alzheimer's Res Ther 2015;7(1):34. https://doi.org/10.1186/s13195-015-0118-1.
[2] Hebert Liesi E, et al. Alzheimer disease in the United States (2010–2050) estimated using the 2010 census. Neurology 2013;80(19):1778–83. https://doi.org/10.1212/WNL.0b013e31828726f5.
[3] Wimo Anders, Jönsson Linus, Bond John, Prince Martin, Winblad Bengt. The worldwide economic impact of dementia 2010. Alzheimer's Dementia 2013;9(1):1–11. https://doi.org/10.1016/j.jalz.2012.11.006.
[4] Krizhevsky Alex, Sutskever Ilya, Geoffrey E. Hinton. Imagenet classification with deep convolutional neural networks. Advances in neural information processing systems. 2016. p. 1097–105.
[5] He Kaiming, Zhang Xiangyu, Ren Shaoqing, Sun Jian. Deep residual learning for image recognition. Proceedings of the IEEE conference on computer vision and pattern recognition. 2016. p. 770–8.
[6] Sabour Sara, Frosst Nicholas, Geoffrey E. Hinton. Dynamic routing between capsules. Adv Neural Inf Process Syst 2017:3856–66.
[7] Worrall Daniel E, et al. Harmonic Networks: Deep Translation and Rotation Equivariance. IEEE Conference on Computer Vision and Pattern Recognition IEEE Computer Society 2017. p. 7168–77. https://doi.org/10.1109/CVPR.2017.758.
[8] Jiménez-Sánchez A, Albarqouni S, Mateus D. Capsule Networks against Medical Imaging Data Challenges. InIntravascular Imaging and Computer Assisted Stenting and Large-Scale Annotation of Biomedical Data and Expert Label Synthesis. Cham: Springer; 2018. p. 150–60. https://doi.org/10.1007/978-3-030-01364-6_17.
[9] Liu Jin, Wang Jianxin, Hu Bin, Wu Fang-Xiang, Pan Yi. Alzheimer's disease classification based on individual hierarchical networks constructed with 3-D texture features. IEEE Trans NanoBioscience 2017;16(6):428–37. https://doi.org/10.1109/TCBB.2017.2731849.
[10] Liu Siqi, Liu Sidong, Cai Weidong, Pujol Sonia, Kikinis Ron, Feng Dagan. Early diagnosis of Alzheimer's disease with deep learning. IEEE 11th International Symposium on Biomedical Imaging ISBI; 2014. p. 1015–8. https://doi.org/10.1109/ISBI.2014.6868045.
[11] Xi E, Bing S, Jin Y. Capsule network performance on complex data. 2017. arXiv preprint arXiv:1712.03480.
[12] Leonardo I. Atrophy Measurement Biomarkers using Structural MRI for Alzheimer's Disease. the 15th Int. Conference on Medical Image Computing and Computer Assisted Intervention. MICCAI; 2012. p. 258.
[13] Grossman M, McMillan C, Moore P, Ding L, Glosser G, Work M, Gee J. What's in a name: voxel-based morphometric analyses of MRI and naming difficulty in Alzheimer's disease, frontotemporal dementia and corticobasal degeneration. Brain 2004;127(3):628–49.
[14] Mizotin M, Benois-Pineau J, Allard M, Catheline G. Feature-based brain MRI retrieval for Alzheimer disease diagnosis. 2012 19th IEEE International Conference on Image Processing. ICIP); 2012. p. 1241–4.
[15] Ashburner J, Friston KJ. Voxel-based morphometry—the methods. Neuroimage 2000;11(6):805–21.
[16] Gerardin E, Chételat G, Chupin M, Cuingnet R, Desgranges B, Kim HS, Niethammer M, Dubois B, Lehéricy S, Garnero L, Eustache F. Multidimensional classification of hippocampal shape features discriminates Alzheimer's disease and mild cognitive impairment from normal aging. Neuroimage 2009;47(4):1476–86.
[17] Cuingnet R, Gerardin E, Tessieras J, Auzias G, Lehéricy S, Habert MO, Chupin M, Benali H, Colliot O. Alzheimer's Disease Neuroimaging Initiative. Automatic classification of patients with Alzheimer's disease from structural MRI: a comparison of ten methods using the ADNI database. Neuroimage 2011;56(2):766–81.
[18] Shen KK, Fripp J, Mériaudeau F, Chételat G, Salvado O, Bourgeat P. Alzheimer's Disease Neuroimaging Initiative. Detecting global and local hippocampal shape changes in Alzheimer's disease using statistical shape models. Neuroimage 2012;59(3):2155–66.
[19] Shaw LM, Vanderstichele H, Knapik-Czajka M, Clark CM, Aisen PS, Petersen RC, Blennow K, Soares H, Simon A, Lewczuk P, Dean R. Cerebrospinal fluid biomarker signature in Alzheimer's disease neuroimaging initiative subjects. Ann Neurol 2009;65(4):403–13.
[20] Liu Y, Paajanen T, Zhang Y, Westman E, Wahlund LO, Simmons A, Tunnard C, Sobow T, Mecocci P, Tsolaki M, Vellas B. Combination analysis of neuropsychological tests and structural MRI measures in differentiating AD, MCI and control groups—the AddNeuroMed study. Neurobiol Aging 2011;32(7):1198–206.
[21] Raut Arpita, Dalal Vipul. A machine learning based approach for detection of Alzheimer's disease using analysis of hippocampus region from MRI scan. IEEE International Conference on Computing Methodologies and Communication ICCMC); 2017. p. 236–42. https://doi.org/10.1109/IST.2017.8261460.
[22] Agarwal M, Mostafa J. Image retrieval for alzheimer's disease detection. MICCAI International Workshop on Medical Content-Based Retrieval for Clinical Decision Support. Berlin, Heidelberg: Springer; 2009. p. 49–60.
[23] Agarwal Mayank, Mostafa Javed. Content-based image retrieval for Alzheimer's disease detection. IEEE, 9th International Workshop on Content-Based Multimedia Indexing CBMI); 2011. p. 13–8. https://doi.org/10.1109/CBMI.2011.5972513.
[24] Akgul CB, Rubin DL, Napel S, Beaulieu CF, Greenspan H, Acar B. Content-based image retrieval in radiology: current status and future directions. J Digit Imag 2011;24(2):208–22.
[25] Fathabad YF, Balafar M. Application of content-based image retrieval in diagnosis brain disease. Int. J. Techn. Phys. Prob. Eng. 2012;4(4):122–8.
[26] Kruthika KR, Pai A, Maheshappa HD. Alzheimer's disease Neuroimaging Initiative. Classification of Alzheimer and MCI Phenotypes on MRI Data Using SVM. International Symposium on Signal Processing and Intelligent Recognition Systems. Cham: Springer; 2017. p. 263–75.
[27] Rabeh Amira Ben, Benzarti Faouzi, Amiri Hamid. Diagnosis of Alzheimer Diseases in Early Step Using SVM (Support Vector Machine). IEEE 13th International Conference on, Computer Graphics, Imaging and Visualization (CGiV) 2016. p. 364–7. https://doi.org/10.1109/CGiV.2016.76.
[28] Farooq Ammarah, Anwar Syed Muhammad, Awais Muhammad, Rehman Saad. A deep CNN based multi-class classification of Alzheimer's disease using MRI. IEEE International Conference on Imaging Systems and Techniques IST); 2017. p. 1–6. https://doi.org/10.1109/IST.2017.8261460.
[29] Hoo-Chang S, Roth HR, Gao M, Lu L, Xu Z, Nogues I, Yao J, Mollura D, Summers RM. Deep convolutional neural networks for computer-aided detection: CNN architectures, dataset characteristics and transfer learning. IEEE Trans Med Imag 2016;35(5):1285. https://doi.org/10.1109/TMI.2016.2528162.
[30] Krizhevsky Alex, Hinton Geoffrey. Learning multiple layers of features from tiny images. Technical report. Univ. Toronto 2009;1(4):7.
[31] Tajbakhsh Nima, Shin Jae Y, Gurudu Suryakanth R, Hurst R Todd, Kendall Christopher B, Gotway Michael B, Liang Jianming. Convolutional neural networks for medical image analysis: Full training or fine tuning? IEEE Trans Med Imag 2016;35(5):1299–312. https://doi.org/10.1109/TMI.2016.2535302.
[32] Suk HI, Lee SW, Shen D. Alzheimer's Disease Neuroimaging Initiative. Latent feature representation with stacked auto-encoder for AD/MCI diagnosis. Brain Struct Funct 2015;220(2):841–59. https://doi.org/10.1007/s00429-013.
[33] Szegedy Christian, Liu Wei, Jia Yangqing, Sermanet Pierre, Scott Reed, Anguelov Dragomir, Erhan Dumitru, Vincent Vanhoucke, Rabinovich Andrew. Going deeper with convolutions. Proceedings of the IEEE conference on computer vision and pattern recognition 2015. p. 1–9. https://doi.org/10.1109/cvpr.2015.7298594.
[34] Zhou Jian, Troyanskaya Olga G. Deep supervised and convolutional generative stochastic network for protein secondary structure prediction. 2014. arXiv preprint arXiv 1403.1347.
[35] Afshar P, Mohammadi A, Plataniotis KN. Brain tumor type classification via capsule networks. 2018. arXiv preprint arXiv 1802.10200.
[36] Mukhometzianov R, Carrillo J. CapsNet comparative performance evaluation for image classification. 2018. arXiv preprint arXiv 1805.11195.
[37] Goodfellow Ian J, Yoshua Bengio, Aaron Courville, Yoshua Bengio. Deep learning vol. 1. Cambridge: MIT press; 2016. https://doi.org/10.4258/hir.2016.22.4.351.
[38] Mitro Joani. Content-based image retrieval tutorial. 2016. arXiv preprint arXiv 1608.03811.
[39] Rueda A, Arevalo J, Cruz A, Romero E, González FA. Bag of features for automatic classification of Alzheimer's disease in magnetic resonance images. Iberoamerican Congress on Pattern Recognition. Berlin, Heidelberg: Springer; 2012. p. 559–66.
[40] Al-Saffar AAM, Tao H, Talab MA. Review of deep convolution neural network in image classification. IEEE 2017, International Conference on Radar, Antenna, Microwave, Electronics, and Telecommunications. ICRAMET; 2017. p. 26–31.
[41] Simonyan K, Zisserman A. Very deep convolutional networks for large-scale image recognition. 2014. arXiv preprint arXiv 1409.1556http://arxiv.org/abs/1409.1556(visited.on.05/02/2018.
[42] McCann MT, Jin KH, Unser M. Convolutional neural networks for inverse problems in imaging: A review. IEEE Signal Process Mag 2017;34(6):85–95. https://doi.org/10.1109/MSP.2017.2739299.
[43] Ilyas Andrew, et al. Query-Efficient Black-box Adversarial Examples. 2017. arXiv preprint arXiv 1712.07113.
[44] Hinton GE, Sabour S, Frosst N. Matrix capsules with EM routing. 2018.

[45] Heung-Il Suk, Shen Dinggang. Deep learning-based feature representation for ad/mci classification. Proceedings of the Medical Image Computing and Computer-Assisted Intervention–MICCAI 2013 Springer; 2013. p. 583–90. https://doi.org/10.1007/978-3-642-40763-5_72.

[46] Zhu Xiaofeng, et al. A novel matrix-similarity based loss function for joint regression and classification in AD diagnosis. Neuroimage 2014;100:91–105. https://doi.org/10.1016/j.neuroimage.2014.05.078.

[47] Zu Chen, et al. Label-aligned multi-task feature learning for multimodal classification of Alzheimer's disease and mild cognitive impairment. Brain Imag. Behav. 2016;10(4):1148–59. https://doi.org/10.1007/s11682-015-9480-7.

[48] Heung-Il Suk, et al. Hierarchical feature representation and multimodal fusion with deep learning for AD/MCI diagnosis. Neuroimage 2014;101:569–82. https://doi.org/10.1016/j.neuroimage.2014.06.077.

[49] Hosseini-asl E, Keynto R, Elbaz A. Alzheimer's Disease Diagnostics by Adaptation of 3D Convolutional Network. IEEE International Conference on Image Processing, Phoenix, Arizona, USA 2016. https://doi.org/10.1109/ICIP.2016.7532332.

[50] Zhang Jun, et al. Detecting Anatomical Landmarks for Fast Alzheimer's Disease Diagnosis. IEEE Trans Med Imag 2016;35(12):2524–33. https://doi.org/10.1109/TMI.2016.2582386.

Update

Informatics in Medicine Unlocked

Volume 20, Issue , 2020, Page

DOI: https://doi.org/10.1016/j.imu.2020.100435

Informatics in Medicine Unlocked 20 (2020) 100435

Contents lists available at ScienceDirect

Informatics in Medicine Unlocked

journal homepage: http://www.elsevier.com/locate/imu

Erratum regarding missing Declaration of Competing Interest statements in previously published articles

Owing to a Publisher error Declaration/Conflict of Interest statements were not included in the published versions of the following articles, that appeared in previous issues of Informatics in Medicine Unlocked.

The appropriate Declaration/Conflict of Interest statements, provided by the Authors, are included below.

1. The relationship between retinal vessel geometrical changes to incidence and progression of Diabetic Macular Edema (Informatics in Medicine Unlocked; 2019; Vol 16C; Article number: 100,248) https://doi.org/10.1016/j.imu.2019.100248

   Declaration of Competing Intere: The Authors have no interests to declare.

2. A machine learning algorithm to improve patient-centric pediatric cardiopulmonary resuscitation (Informatics in Medicine Unlocked; 2020; Vol 19C; Article number: 100,339) https://doi.org/10.1016/j.imu.2020.100339

   Declaration of interest: The Authors have no interests to declare.

3. Decision support system for diagnosing Rheumatic-Musculoskeletal Disease using fuzzy cognitive map technique (Informatics in Medicine Unlocked; 2019; Vol 18C; Article number: 100,279) https://doi.org/10.1016/j.imu.2019.100279

   Declaration of interest: The Authors have no interests to declare.

4. Channel binary pattern based global-local spatial information fusion for motor imagery tasks (Informatics in Medicine Unlocked; 2020; Vol 20C; Article number: 100,352) https://doi.org/10.1016/j.imu.2020.100352

   Declaration of interest: The Authors have no interests to declare.

5. Classification of malignant and benign tissue with logistic regression (Informatics in Medicine Unlocked; 2019; Vol 16C; Article number: 100,189) https://doi.org/10.1016/j.imu.2019.100189

   Declaration of interest: The Authors have no interests to declare.

6. On parameter interpretability of phenomenological-based semi-physical models in biology (Informatics in Medicine Unlocked; 2019; Vol 15C; Article number: 100,158) https://doi.org/10.1016/j.imu.2019.02.002

   Declaration of interest: The Authors have no interests to declare.

7. Multistage Classifier-Based Approach for Alzheimer's Disease Prediction and Retrieval (Informatics in Medicine Unlocked; 2018 vol 14C; Pages 34–42) https://doi.org/10.1016/j.imu.2018.12.003

   Declaration of interest: The Authors have no interests to declare.

8. A novel somatic cancer gene based biomedical document feature ranking and clustering model (Informatics in Medicine Unlocked; 2019; Vol 16C; Article number: 100,188) https://doi.org/10.1016/j.imu.2019.100188

   Declaration of interest: The Authors have no interests to declare.

9. Developing an ultra-efficient microsatellite discoverer to find structural differences between SARS-CoV-1 and Covid-19 (Informatics in Medicine Unlocked; 2020 vol 19C; Article number: 100,356) https://doi.org/10.1016/j.imu.2020.100356

   Declaration of interest: The Authors have no interests to declare.

10. Patient-specific optimization of mechanical ventilation for patients with acute respiratory distress syndrome using quasi-static pulmonary P–V data (Informatics in Medicine Unlocked; 2018;

DOIs of original article: https://doi.org/10.1016/j.imu.2020.100352, https://doi.org/10.1016/j.imu.2020.100356, https://doi.org/10.1016/j.imu.2019.100248, https://doi.org/10.1016/j.imu.2018.12.003, https://doi.org/10.1016/j.imu.2019.100177, https://doi.org/10.1016/j.imu.2019.100189, https://doi.org/10.1016/j.imu.2019.100256, https://doi.org/10.1016/j.imu.2020.100339, https://doi.org/10.1016/j.imu.2019.100279, https://doi.org/10.1016/j.imu.2019.100188, https://doi.org/10.1016/j.imu.2019.100171, https://doi.org/10.1016/j.imu.2018.06.003, https://doi.org/10.1016/j.imu.2018.12.001, https://doi.org/10.1016/j.imu.2020.100308, https://doi.org/10.1016/j.imu.2019.100184, https://doi.org/10.1016/j.imu.2019.02.002, https://doi.org/10.1016/j.imu.2020.100304.

https://doi.org/10.1016/j.imu.2020.100435

Available online 28 September 2020

Vol 12C; Pages 44–55) https://doi.org/10.1016/j.imu.2018.06.003

Declaration of interest: The Authors have no interests to declare.

11. A technology framework for remote patient care in dermatology for early diagnosis (Informatics in Medicine Unlocked; 2019; Vol 15C; Article number: 100,171) https://doi.org/10.1016/j.imu.2019.100171

Declaration of interest: The Authors have no interests to declare.

12. CBIR System Using Capsule Networks and 3D CNN for Alzheimer's disease Diagnosis (Informatics in Medicine Unlocked; 2018; Vol 14C; Pages 59–68) https://doi.org/10.1016/j.imu.2018.12.001

Declaration of interest: The Authors have no interests to declare.

13. The effect of computerized physician order entry on mortality rates in pediatric and neonatal care setting: Meta-analysis (Informatics in Medicine Unlocked; 2020; Vol 19C; Article number: 100,308) https://doi.org/10.1016/j.imu.2020.100308

Declaration of interest: The Authors have no interests to declare.

14. Identification of the core ontologies and signature genes of polycystic ovary syndrome (PCOS): A bioinformatics analysis. (Informatics in Medicine Unlocked; 2020; Vol 18C; Article number: 100,304) https://doi.org/10.1016/j.imu.2020.100304

Declaration of interest: The Authors have no interests to declare.

15. Balanites aegyptiaca (L.) Del. for dermatophytoses: Ascertaining the efficacy and mode of action through experimental and computational approaches (Informatics in Medicine Unlocked; 2019; Vol 15C; Article number: 100,177) https://doi.org/10.1016/j.imu.2019.100177

Declaration of interest: The Authors have no interests to declare.

16. Barriers and technologies of maternal and neonatal referral system in developing countries: A narrative review (Informatics in Medicine Unlocked; 2019; Vol 15C; Article number: 100,184) https://doi.org/10.1016/j.imu.2019.100184

Declaration of interest: The Authors have no interests to declare.

17. Automated Grading of Prostate Cancer using Convolutional Neural Network and Ordinal Class Classifier (Informatics in Medicine Unlocked; 2019; Vol 17C; Article number: 100,256) https://doi.org/10.1016/j.imu.2019.100256

Declaration of interest: The Authors have no interests to declare.